FUDMA Journal of Sciences (FJS)
ISSN online: 2616-1370
ISSN print: 2645 - 2944
Vol. 7 No. 3, June, 2023, pp 112 - 124
DOI: https://doi.org/10.33003/fjs-2023-0703-1828

EXPLORING THE DYNAMICS OF AN EXOTHERMIC CHEMICAL REACTION CONTROLLED BY ARRHENIUS KINETICS WITH HALL EFFECT IN A MICROCHANNEL

[1]Hamza M. M., [1]Ahmad S. K., *[2]Ojemeri G., [1]Usman H. and [2]Shuaibu A.

[1]Department of Mathematics, Faculty of Physical and Computing Sciences, Usmanu Danfodiyo University, P. M. B. 2346, Sokoto.
[2]Department of Mathematics, College of Sciences, Federal University of Agriculture, P.M. B. 28, Zuru, Kebbi State.

*Corresponding authors' email: godwinojemeri@gmail.com

ABSTRACT
The consequences of chemically reactive fluids have provoked many researchers due to their potential to enhance the behavior of heat. Hence, this article discussed a theoretical investigation to explore the actions of Arrhenius chemical reaction and Hall current on hydro-magnetic free convection of a viscous fluid flowing along an upstanding micro-channel. Subject to the required boundary conditions, the governing coupled equations representing the flow pattern in non-dimensional form were solved using the homotopy perturbation method (HPM). Line graphs are also used to generate expressions for energy, momentum, volume flow rate, drag force, and Nusselt number in both primary and secondary flow directions as a function of regulating parameters like chemical reaction, Hall current, rarefaction, and wall ambient temperature difference ratio. It is worthy of note that the fluid temperature and the fluid flow are substantially propelled by the viscous heating term in the Arrhenius chemical reaction of the system for growing values of the wall ambient temperature difference ratio parameter. Additionally, it is noticeable that volume flow rate performance is seen as a growing influence of viscous heating and rarefaction parameters. The findings of this study can be applied to a wide range of electrically controlled devices, thermal and petro chemical engineering, and the serviceability of industrial products.

Keywords: Hall effect, Arrhenius kinetics, Rarefaction, Micro-channel, Homotopy perturbation method (HPM)

INTRODUCTION

The phenomena of Hall effects appear when the introduced magnetic factor is extremely strong or when partly ionized gases have a high cyclotron frequency. Most of the electricity generated in a fluid is propelled by electrons, which repeatedly collide with other energized particles and are often more unsteady than ions. Because of the rapid movement and randomness of the charged particles, the conductivity parallel to the electric field decreases, and current is induced in the direction perpendicular to both the electric and magnetic fields. This occurrence is defined as the "Hall Effects." Magneto-hydrodynamics (MHD) flows having Hall currents have engineering applications such as Hall accelerations, power generators, turbine construction, and centrifugal machines (Sutton and Sherman, 1965, Quader and Alam, 2021). In light of this, Urgun *et al*. (2022) discussed the analytical simulation of Von Karman flow and MHD heat transmission of an electrically conducting fluid influenced by Hall Effect through an infinitely radially shrinking rotating disk. Jha and Malgwi (2021) have published a paper on the role of conducting and non-conducting surfaces on the hydro magnetic free convection of viscous fluid along an upstanding micro-channel in the coexistence of Hall current and induced magnetic number. Krishna *et al*. (2020) evaluated the actions of Hall and ion slip currents on the time-dependent rotating flow of a conducting fluid having porosity effect. It was concluded that the presence of a magnetic number impedes flow reversal and that the inclined angle has a declining influence on fluid velocity. Krishna et al. (2020) then described the hydro-magnetic rotating flow of microscopic creature propulsion across a permeability medium in the coexistence of Hall and ion slip condition. It was discovered that the magnetic number, Darcy porous parameter, Hall parameter, and ion slip parameter all play vital roles in fluid flow characteristics. The combined effects of Dufour effect, radiation-absorption, and Hall and ion slip flow on the hydro magnetic free convective circulatory flow of nano-fluids (Ag and TiO_2) across a semi-infinite porous non stationary plate with uniform heat emission were explored by Krishna and Chamkha (2019). Their findings reveal that increasing the rotation parameter reduces velocity while increasing the Hall and ion slip conditions and the Dufour effect increases velocity. In another article, Jha and Malgwi (2019) reported the actions of Hall conditions and induced magnetic number on steady hydro magnetic convection in a micro-channel subjected to an inclined magnetic field. Their computational analysis revealed that magnetic field inclination plays a substantial role on the flow characteristics in the micro-channel. Rajput and Gupta (2021) explored the effects of Hall current and thermal radiation on transient free hydro magnetic flow with an inclined magnetic field. The key findings of their computational research revealed that the Hall Effect significantly increase both the primary and secondary flow distributions. Magnetic fields and thermal radiation, on the other hand, tend to boost secondary velocity while decreasing primary velocity. Jha *et al*. (2017) stressed the impact of Hall current on MHD convection in a micro-channel limited to two immeasurable upstanding parallel plates restricted to unequal heating. The study's key findings demonstrated that higher levels of Hall current and rarefaction characteristics increase the volume flow rate.

In view of the numerous cooling functions in processing activities and fabrication, including micro-heat pipes, aerospace and high-power density chips in supercomputers and other devices, there has been an upsurge in interest in microfluidics and heat transfer in recent years. Comprehending the flow configuration is becoming extremely significant for exact modelling predictions since

the bulk of these structures involve internal micro-channel flows (Al-Nimr and Khadrawi 2004, Jha et al. 2014a). To this end, Hamza et al. (2023) recently highlighted an analytical investigation on the effect of Arrhenius chemical reaction due to an induced magnetic field in a microchannel. Jha and Aina (2016) discussed the hydro magnetic convection in a micro-channel confined to two electrically non-conducting immeasurable upstanding plates. Ltaifa et al. (2021) carefully investigated heat transfer in a rectangular inclined micro-channel immersed with a water/Al2O3 nanofluid. Other references include (Chen and Weng 2005, Jha and Aina 2015, Buonomo and Manca, 2012, Weng and Chen 2009, Jha et al. 2015, Jha et al. 2014b).

The in-depth investigation of magneto-hydrodynamics (MHD) flow phenomenon is crucial and has attracted great intellectual curiosity attributable to its possible advantages in a number of industrial and engineering fields, like in MHD generators, fusion reactors, electric transformers, optical grafting, metal casting, crystal growth, MHD accelerators and metallurgical processes. Additionally, chemical energy technology already uses MHD pumps for propelling electrically conductive fluids in a number of atomic energy structures. Besides contributing to these uses, an applied magnetic field may profoundly improve free convection when the fluid is electrically charged (Zainal *et al*. 2021, Jha *et al.* 2015). Numerous investigations of MHD convection flows in several physical conditions have been performed. Ojemeri *et al*. (2023) recently inspected the steady MHD flow of an electrically conductive Casson fluid controlled by radiation effect in an upstanding porous channel. Applying the finite difference method (FDM), Omokhuale & Dange (2023) numerically analyzed the action of heat sink on time-dependent MHD Jeffery flow of a chemically reactive fluid. Hamza and Shuaibu (2022) deliberated on MHD convection of an exothermic chemical reaction affected by Newtonian heating in an upstanding channel. Ojemeri and Hamza (2022) proposed an analytical investigation of an Arrhenius kinetically affected by heat source/sink fluid with MHD effect in a microchannel. Gul *et al*. (2021) highlighted the hybrid nanofluid function on hydro magnetic boundary layer flow for a chemically reacting fluid in light of this. Saeed and Gul (2021) researched the hydro magnetic Casson nanofluid flow with heat and mass transfer along a non-stationary plate. Ziz and Shams (2020) carried out the entropy generation in the hydro magnetic Maxwell nanofluid flow affected by slip condition, thermal generation, and variable thermal conductivity. Guriviredy et al. (2016), employed a semi-infinite non stationary upstanding porous plate with Soret factor to analyze the impacts of heat generation and chemical reactions on hydro magnetic flow. El-Aziz and Yahaya (2017) discussed the heat and mass transfer coefficient of a time-dependent hydro magnetic flow saturated with porosity effect across an upstanding plate with uniform layer heat condition.

The equations governing the current flow problem are nonlinear and coupled, making it challenging to derive closed-form solutions. As a result, numerical schemes or approximate solution procedures can be used to tackle such problems. One of the most efficient approaches is the perturbation method. The perturbation method's solutions, on the other hand, are confined to small perturbation parameters. Another method, known as the homotopy perturbation method, was developed to overcome this limitation. He (1999) utilized the method to solve partial or ordinary forms that are linear, nonlinear, or coupled equations. He investigated a nonlinear coupling method using a homotopy and a perturbation procedure (He 2000 and He 2006). Later, He (2003) presented a new nonlinear analytical methodology based on homotopy perturbation.

A closer look into the above-mentioned literature, however reveals a knowledge gap; the influence of chemically reactive fluid has not been considered, probably for the reason of having a simplified mathematical formulation. However, this effect is particularly significant due its relevance in emerging MEMS, engineering sciences and lubrication industries, since most of the lubricants used in engineering and industrial activities, like synthetic esters, hydrocarbon oils, polyglycols, are reactive. Therefore, the main target of this research is to build on the model of Jha *et al*. (2017) by incorporating the action of Arrhenius chemical reaction on steady free convection in an upstanding micro-channel affected by Hall effect confined by two immeasurable upstanding parallel plates subjected to unequal heating of the plates using the homotopy perturbation technique. The uniqueness of this work is that it utilizes HPM to establish some approximate solutions for a chemically reacting fluid regulated by Arrhenius kinetics between two vertical microchannel walls. This research is also motivated by the increased quest for various industrial working fluids and earlier researches on the relevance of Arrhenius energy and exothermic chemical reactions in chemical engineering, biotechnology, food processing, thermal sciences, and other fields.

Problem formulation

Under the consequences of the Hall Effect, the steady free convection of an Arrhenius-driven fluid in a vertical micro-channel restricted to two electrically non-conducting immeasurable upstanding plates is investigated with an applied magnetic field. The x-axis is normal to the gravitational force g but in the reverse direction, while the y-axis is orthogonal to the upward plate. The flow configuration is portrayed in Figure 1. A unaltered magnetic strength of B_0 is assumed to be applied in the path normal to the flow movement. Also, it is assumed that the magnetic Reynolds number is negligible, meaning that the produced magnetic field is little in contrast to the one introduced externally. The surfaces are heated unequally, with one plate retained at T_1 and the other at T_2, with $T_1 > T_2$. Free convection in the microchannel is due to the temperature variance between the plates and the reactive nature of the fluid. The following assumptions are used to formulate this problem:

i. Unlike buoyancy, the horizontal magnetic field has a considerable impact.
ii. A uniform magnetic field B0 is provided perpendicular to the flow direction while ignoring the induced magnetic fields by assuming a very tiny magnetic Reynolds number.
iii. The influence of the Frank-Kamenetskii parameter is taken into account.
iv. The impact of Joule heating is neglected in favor of viscous dissipation.

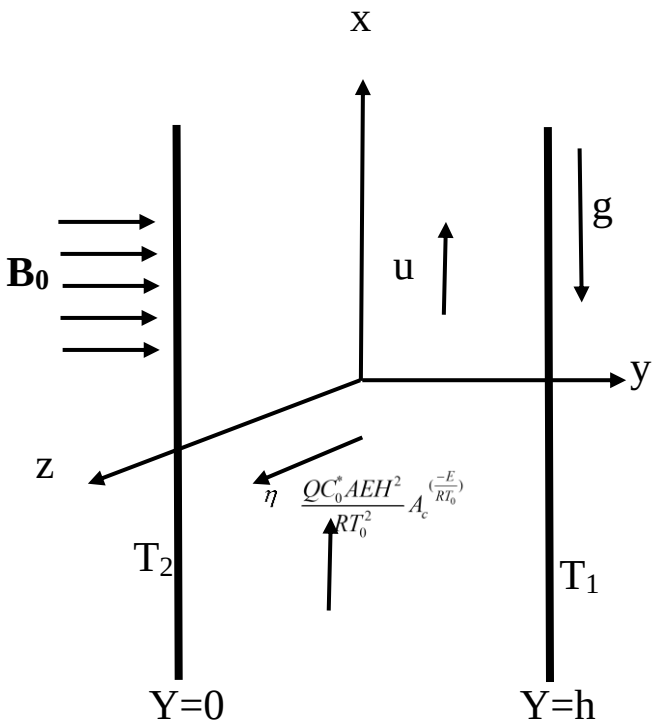

Figure 1: Physical coordinate of the flow domain

The momentum and temperature equations for this particular physical problem are provided in non-dimensional form in accordance with Jha et al. (2017) and Ojemeri and Hamza (2022), with the fundamental idea of Boussinesq's approximation.

Velocity equation

$$\frac{d^2U}{dY^2} - \frac{M^2}{(1+N_p^2)}(U + N_p\eta) = -\theta \tag{1}$$

Induced magnetic field

$$\frac{d^2\eta}{dY^2} + \frac{M^2}{(1+N_p^2)}(N_pU - \eta) = 0 \tag{2}$$

Temperature equation

$$\frac{d^2\theta}{dY^2} + K_r e^{\frac{\theta}{1+A_c\theta}} = 0 \tag{3}$$

The boundary conditions at the microchannel walls are as follows;

$$\left.\begin{aligned} U(Y) = \beta_v Kn\frac{dU}{dY}, \eta(Y) = \beta_v Kn\frac{d\eta}{dY}, \theta(Y) = \xi + \beta_v KnIn\frac{d\theta}{dY}, \ at \quad Y = 0 \\ U(Y) = -\beta_v Kn\frac{dU}{dY}, \eta(Y) = -\beta_v Kn\frac{d\eta}{dY}, \theta(Y) = 1 - \beta_v KnIn\frac{d\theta}{dY}, \ at \quad Y = 1 \end{aligned}\right\} \tag{4}$$

Where Np is the Hall current, M is the magnetic number, K_r is the Frank–Kamenetskii parameter and A_c is the activation energy. It is useful to clarify that, in the expansion of heat source term $K_r(1 + A_c\theta)^m e^{\frac{\theta}{1+A_c\theta}}$, the Arrhenius heating case (i.e. when m = 0) was investigated in this research.

The dimensionless parameters employed in the flow configuration are described below:

$$\beta_v = \frac{2-f_v}{f_v}, \beta_t = \frac{2-f_t}{f_t}\frac{2\gamma_s}{\gamma_s+1}\frac{1}{Pr\frac{a}{b}\frac{\beta_t}{\beta_v}\frac{T_2-T_0}{T_1-T_0}}$$

$$Y = \frac{y}{b}, \theta = \frac{T-T_0}{T_1-T_0}, M^2 = \frac{\sigma\mu_e^2B_0^2b^2}{\rho v}, Pr = \frac{v}{\alpha}, (U,\eta) = \frac{(u,\eta)v}{g\beta\Delta Tb^2} \tag{5}$$

$$A_c = \frac{RT_0}{E}, K_r = \frac{QC_0^*AEH^2}{RT_0^2}A_c^{(\frac{-E}{RT_0})}, N_p = \omega_e\tau_e$$

Solution of the problem

Homotopy Perturbation Method (HPM)

The closed form expressions for the nonlinear ordinary differential equations have been obtained. To resolve our current model, HPM have been employed. Convex homotopy on the coupled nonlinear lead equations (1-3) has been formulated. The equations now become:

$$H(U,p) = (1-p)\frac{d^2U}{dY^2} - p\left[\frac{M^2}{(1+N_p^2)}(U + N_p\eta) - \theta\right] = 0 \quad (6)$$

$$H(\eta,p) = (1-p)\frac{d^2\eta}{dY^2} + p\left[\frac{M^2}{(1+N_p^2)}(N_pU - \eta)\right] = 0 \quad (7)$$

$$H(\theta,p) = (1-p)\frac{d^2\theta}{dY^2} + p\left[K_r e^{\frac{\theta}{1+A_c\theta}}\right] = 0 \quad (8)$$

Given that the solutions ofθ, η and U is in an infinite series form as:

$$\left.\begin{aligned}\theta(Y) &= \theta_0 + p\theta_1 + p^2\theta_2 + \dots\\ \eta(Y) &= \eta_0 + p\eta_1 + p^2\eta_2 + \dots\\ U(Y) &= u_0 + pu_1 + p^2u_2 + \dots\end{aligned}\right\} \quad (9)$$

Substituting equation (9) into equations (6), (7) and (8), and comparing the coefficient of like powers p, we obtain the solutions to the temperature and velocity as follows:

$$\theta_0 = A_0 + A_1Y \quad (10)$$

$$\theta_1 = -K_r\left[\ \frac{Y^2}{2} + A_0\frac{Y^2}{2} + A_1\frac{Y^3}{6} + (2-A_c)\left(A_0^2\frac{Y^2}{2} + A_0A_1\frac{Y^3}{3} + A_1^2\frac{Y^4}{12}\right)\ \right] + A_3Y + A_2 \quad (11)$$

$$\begin{aligned}\theta_2 = -(4K_r - 2A_cK_r)\Bigg[K_r\{&A_0\frac{Y^4}{24} + A_0^2\frac{Y^4}{24} + A_0A_1\frac{Y^5}{120} + (2-A_c)\left(A_0^3\frac{Y^4}{24} + A_0^2A_1\frac{Y^5}{60} + A_0A_1^2\frac{Y^6}{360}\right)\ \}\\ &+A_0A_3\frac{Y^3}{6} + A_0A_2\frac{Y^2}{2} - K_r\Bigg\{A_1\frac{Y^5}{40} + A_0A_1\frac{Y^5}{40} + A_1^2\frac{Y^6}{180} + (2-A_c)\left(A_0^2A_1\frac{Y^5}{40} + A_0A_1^2\frac{Y^6}{60} + A_1^3\frac{Y^7}{504}\right)\ \}\\ &+A_3A_1\frac{Y^4}{12} + A_2A_1\frac{Y^3}{6}\ \Bigg] + {K_r}^2\Bigg\{\frac{Y^4}{24} + A_0\frac{Y^4}{24} + A_1\frac{Y^5}{120} + (2-A_c)\left(A_0^2\frac{Y^4}{24} + A_0A_1\frac{Y^5}{60} + A_1^2\frac{Y^6}{360}\right)\ \}\end{aligned}$$

$$+K_r\left(A_3\frac{Y^3}{6} + A_2\frac{Y^2}{2}\right) + A_5Y + A_4 \quad (12)$$

$$u_0 = R_1\frac{Y^3}{6} + R_2\frac{Y^2}{2} + R_3Y + R_4 \quad (13)$$

$$u_1 = 2w_1\left(\frac{R_1Y^5}{120} + \frac{R_2Y^4}{24}\right) - w_2\left(\frac{R_1Y^7}{5040} + \frac{R_2Y^6}{720} + \frac{R_3Y^5}{120} + \frac{R_4Y^4}{120}\right) + w_1\left(A_0\frac{Y^4}{24} + A_1\frac{Y^5}{120}\right)$$

$$+R_5\frac{Y^3}{6} + R_6\frac{Y^2}{2} + R_7Y + R_8 \quad (14)$$

$$\eta_0 = \frac{1}{N_pw_1}(R_1Y + R_2) + \frac{1}{N_pw_1}(A_0Y + A_1) - \frac{1}{N_p}\left(R_1\frac{Y^3}{6} + R_2\frac{Y^2}{2} + R_3Y + R_4\right) \quad (15)$$

$$\begin{aligned}\eta_1 = &\frac{1}{N_pw_1}\left[2w_1\left(\frac{R_1Y^3}{6} + \frac{R_2Y^2}{2}\right) - w_2\left(\frac{R_1Y^5}{120} + \frac{R_2Y^4}{24} + \frac{R_3Y^3}{6} + \frac{R_4Y^2}{2}\right) + w_1\left(A_0\frac{Y^2}{2} + A_1\frac{Y^3}{6}\right) + R_5Y + R_6\right]\\ &+\frac{1}{N_pw_1}\left[-\lambda\left[\ \frac{Y^2}{2} + A_0\frac{Y^2}{2} + A_1\frac{Y^3}{6} + (2-A_c)\left(A_0^2\frac{Y^2}{2} + A_0A_1\frac{Y^3}{3} + A_1^2\frac{Y^4}{12}\right)\ \right] + A_3y + A_2\right]\\ -\frac{1}{N_p}&\left[\begin{aligned}&2w_1\left(\tfrac{R_1Y^5}{120} + \tfrac{R_2Y^4}{24}\right) - w_2\left(\tfrac{R_1Y^7}{5040} + \tfrac{R_2Y^6}{720} + \tfrac{R_3Y^5}{120} + \tfrac{R_4Y^4}{120}\right) + w_1\left(A_0\tfrac{Y^4}{24} + A_1\tfrac{Y^5}{120}\right)\\ &+R_5\tfrac{Y^3}{6} + R_6\tfrac{Y^2}{2} + R_7Y + R_8\end{aligned}\right]\end{aligned} \quad (16)$$

Setting p to be 1, the solutions of the differential equations in the approximate form becomes

$$\left.\begin{aligned}\boldsymbol{\theta(Y)} &= \boldsymbol{\theta_0 + \theta_1 + \theta_2 + \dots}\\ \boldsymbol{U(Y)} &= \boldsymbol{u_0 + u_1 + u_2 + \dots}\\ \boldsymbol{\eta(Y)} &= \boldsymbol{\eta_0 + \eta_1 + \eta_2 + \dots}\end{aligned}\right\} \quad \mathbf{(17)}$$

The series in equations (17) typically converges even for few terms. On the other hand, the nonlinear operator determines the rate of convergence. Ayati and Biazar (2015) assert that just a few terms of the homotopy perturbation procedure can be utilized to get an approximative solutions that converges to the series solution.

Defining the complex velocity as $\varphi = U + i\eta$, eqs (1) and (2) now becomes

$$\frac{d^2\phi}{dY^2} - M_1^2\phi = -\theta \quad (18)$$

$$where M_1^2 = \frac{M^2}{(1+iN_p)}$$

The boundary condition is given as

$$\left.\begin{aligned}\phi(Y) = \beta_vKn\frac{d\phi}{dY}, \theta(Y) &= \xi + \beta_vKnIn\frac{d\theta}{dY}, \quad at \qquad Y = 0\\ \phi(Y) = -\beta_vKn\frac{d\phi}{dY}, \theta(Y) &= 1 - \beta_vKnIn\frac{d\theta}{dY}, \quad at\ Y = 0\end{aligned}\right\} \quad (19)$$

Constructing homotopy on eqs (18) and (19) and assuming the solution of the complex velocity to be

$\phi = \phi_0 + p\,\phi_1 + p^2\,\phi_2 + \ldots$

We obtain the appoximate solution of ϕ as:

$$\phi_0 = J_0 Y + J_1 \tag{20}$$

$$\phi_1 = -A_1\frac{Y^3}{6} - A_0\frac{Y^2}{2} + J_2 Y + J_3 \tag{21}$$

$$\phi_2 = M_1^2\left(-A_1\frac{Y^5}{120} - A_0\frac{Y^4}{24} + J_3\frac{Y^3}{6} + J_4\frac{Y^2}{2}\right) + K_r\left[\frac{Y^4}{24} + A_0\frac{Y^4}{24} + A_1\frac{Y^5}{120} + (2-A_c)(A_0^2\frac{Y^4}{24} + A_0A_1\frac{Y^5}{60} + A_1^2\frac{Y^6}{360})\right] - A_3\frac{Y^3}{6} - A_2\frac{Y^2}{2} + J_4 Y + J_5 \tag{22}$$

Also, letting p to be 1, the solutions of the complex velocity is derived as:

$$\phi = \lim_{p\to 1}\phi = \phi_0 + \phi_1 + \phi_2 + \ldots \Big\} \tag{23}$$

Two phenomena that are crucial for buoyancy-driven microchannel flows are the rate of volume flow (Γ) and the skin friction (τ). The complex volume flow rate is given as:

$$\Gamma = \phi_x + i\phi_z; where \phi_x = Re(\Gamma), and i\phi_z = Im(\Gamma)$$

$$\Gamma = \int_0^1 \phi\, dY \tag{24}$$

$$\Gamma = \int_0^1 \begin{bmatrix} -A_1\frac{Y^3}{6} - A_0\frac{Y^2}{2} + J_2 Y + J_3 + M_1^2\left(-A_1\frac{Y^5}{120} - A_0\frac{Y^4}{24} + J_3\frac{Y^3}{6} + J_4\frac{Y^2}{2}\right) \\ +K_r\left[\frac{Y^4}{24} + A_0\frac{Y^4}{24} + A_1\frac{Y^5}{120} + (2-A_c)(A_0^2\frac{Y^4}{24} + A_0A_1\frac{Y^5}{60} + A_1^2\frac{Y^6}{360})\right] - A_3\frac{Y^3}{6} - A_2\frac{Y^2}{2} + J_4 Y + J_5 \end{bmatrix} dY \tag{25}$$

$$\Gamma = -\frac{A_1}{24} - \frac{A_0}{6} + \frac{J_2}{2} + J_3 + M_1^2\left(-\frac{A_1}{720} - \frac{A_0}{120} + \frac{J_2}{24} + \frac{J_3}{6}\right) + K_r\left[\frac{1}{120} + \frac{A_0}{120} + \frac{A_1}{720} + (2-A_c)(\frac{A_0^2}{120} + \frac{A_0A_1}{360} + \frac{A_1^2}{2520})\right] - \frac{A_3}{24} - \frac{A_2}{6} + J_5 + \frac{J_4}{2} + J_5 \tag{26}$$

Steady state frictional force (τ) at Y=0 and Y=1 at both plates for primary and secondary flows is obtained as:

$$\tau_{x0} + i\tau_{z0} = \left.\frac{d\phi}{dY}\right|_{Y=0} = J_2 + J_4 \tag{27}$$

$$\tau_{x1} + i\tau_{z1} = \left.\frac{dU}{dY}\right|_{Y=1} = -\frac{A_1}{2} - A_0 + J_2 + M_1^2(-\frac{A_1}{24} - \frac{A_0}{6} + \frac{J_2}{2} + J_3) + K_r(\frac{1}{24} + \frac{A_0}{6} + \frac{A_1}{24}) + (2-A_c)(\frac{A_0^2}{6} + \frac{A_0A_1}{12} + \frac{A_1^2}{60}) - \frac{A_3}{2} - A_2 + J_4 \tag{28}$$

While the heat transfer coefficient at both microchannel plates is obtained as:

$$Nu_0 = \frac{qb}{(T_1 - T_0)k} = \left.\frac{d\theta}{dY}\right|_{Y=0} = A_1 + A_3 + A_5 \tag{29}$$

$$Nu_1 = \frac{qb}{(T_1 - T_0)k} = \left.\frac{d\theta}{dY}\right|_{Y=1} = A_1 - k_r\left[1 + A_0 + \frac{A_1}{2} + (2-A_c)(A_0^2 + A_0A_1 + \frac{A_1^2}{3})\right] + A_3 - (4k_r - 2A_ck_r)\left[\frac{A_0}{6} + \frac{A_0^2}{6} + \frac{A_0A_1}{24}\right.$$
$$(2-A_c)(\frac{A_0^3}{6} + \frac{A_0^2A_1}{12} + \frac{A_0A_1^2}{60}) + \frac{A_0A_3}{2} + A_0A_2 - k_r\left\{\frac{A_1}{8} + \frac{A_0A_1}{8} + \frac{A_1^2}{60}\right.$$
$$+(2-A_c)(\frac{A_0^2A_1}{8} + \frac{A_1^2A_0}{10} + \frac{A_1^3}{72}) \quad \} + \frac{A_3A_1}{3} + \frac{A_0A_1}{2} \quad] + {k_r}^2\left\{\frac{1}{6} + \frac{A_0}{6} + \frac{A_1}{24} + \right.$$
$$(2-A_c)(\frac{A_0^2}{6} + \frac{A_0A_1}{12} + \frac{A_1^2}{60}) \quad \} + k_r(\frac{A_3}{2} + A_2) + A_5 \tag{30}$$

DISCUSSION OF RESULTS

This section is devoted to showcasing the deviations of the fluid parameters such as viscous heating term (K_r), activation energy (A_c), wall-ambient temperature difference ratio (ξ), rarefaction parameter ($\beta_v Kn$) and Hall current (Np) on free convection and heat transfer flow employing the homotopy perturbation method (HPM) in a vertical microchannel. The deviation of temperature, primary velocity (U), secondary velocity (η), volume flow rate, sheer stress and heat transfer amount are described in Figures 2-12 to illustrate the impacts of these regulating factors. The present research was done in the continuum and slip flow region (Kn≤0.1) over meaningful interval of $0 \leq \beta_v Kn \leq 0.1$, $1 \leq Np \leq 2$ and $0 \leq In \leq 10$. The product of $\beta_v Kn$ show a level of departure from the continuum regime, and (In) implies a fluid-wall interaction factor. For this analysis, the selected default values for ($\beta_v Kn$) and (In) are 0.05 and 1.667, respectively, as employed by Chen and Weng (2005), and M=2 as used by Jha et al. (2014a) in addition, the reference values taken for this computations are K_r=0.1, Np=1. M=2, $\beta_v Kn$ =0.05, In=1.667 and A_c=0.01 to elucidate the influence of various flow characteristics.

Figure 2 show the impacts of chemical reaction parameter (K_r), also known as viscous heating parameter, rarefaction parameter ($\beta_v Kn$) and wall-ambient temperature difference ratio (ξ) on the temperature gradient under three cases of the wall- ambient temperature difference ratio (ξ = -1: one heating and one cooling; ξ = 0: one heating and one not heating, ξ =1: both walls are heated). It is abundantly obvious that when the values of K_r and $\beta_v Kn$ grow, the temperature jump increases significantly, notably in the region of the left proximity of the micro-channel. This is naturally true because uplifting the viscous heating term yields a minimization in the drag force, consequently weakening the flow resistance. The size of the viscous heating sources in energy equations is encouraged as fluid motion rises, leading to a stronger fluid temperature.

Figure 3 depict the pattern of K_r and (ξ) on the velocity profile. A close examination at this figure reveals that both the primary and secondary flows are moving upward, notably towards the center of the micro-channel, as K_r and $\beta_v Kn$ are increased. In the case of the primary velocity, these impacts are more pronounced. We observed that with greater levels of reaction rate parameter K_r drastically instigate the exothermic chemical reaction and substantially boost the fluid movement due to the temperature spike. Naturally speaking, the exothermic chemical reactions causes an upsurge in the heat generation due to growing levels of K_r. Moreover, the speeds of Arrhenius provoked reactions encourages internal heat enhancement.

Figure 4a and b describe the influence of $\beta_v Kn$ and (ξ) on the primary and secondary velocity. The fluid velocity is increased in both the primary and secondary directions when the levels of rarefaction and the wall ambient temperature differential ratio are increased. This effect can be described from the fact that when the rarefaction parameter grows, the temperature rises as well, reducing the amount of heat transferred from the walls to the fluid. The strengthening in the fluid motion caused by the petering out in the diminishing drag forces close to the surfaces make up for the reduction in fluid flow initiated by reducing the impact on the amount of heat transport. It's worth noting that in the case of the primary velocity, these affects are more evident.

The functions of Np and (ξ) on both the primary and secondary flows are demonstrated in Fig. 5a and b. It is clear that mounting values of Np and (ξ) respectively causes a substantial growth in both the primary and secondary velocity, with the effects being more obvious in the case of the secondary velocity. Further, raising the Hall current parameter tends to reduce the magnetic field effect on the complex velocity, resulting in the upsurge in both the primary and secondary velocities.

The flow pattern for the volume flow rate as K_r vary is depicted in Fig. 6. It is plain that uplifting the values of K_r against $\beta_v Kn$, the primary and secondary flows rises at the micro-channel walls. It is shown that, a rise in the level of rarefaction parameter encourages a strengthening in the volume flow amount. In addition, it is clearly noticeable that the chemical reaction parameter is seen to boost up the rate of volume flow.

The plots for frictional forces at both plates affected by K_r is illustrated in Figs. 7 and 8. As seen from Figs. 7a and b, at different growing levels of (ξ), the skin friction is noticed to reduce for an increasing function of K_r at Y=0, whereas a counter attribute is evident at Y=1 as portrayed in Figs 8a and b. The actions of (K_r) versus ($\beta_v Kn$) on the heat transmission rate is plotted in Fig. 9. It is worthy of mentioning that an observable growth in the heat transfer rate is stronger as K_r and $\beta_v Kn$ rise respectively in the plate (Y=0), as noticed in Figure 9a, while at Y=1, an opposite behavior is established as depicted in Fig. 9b. This is so because strengthening (reducing) fluid temperature encourages (slows down) the exothermic chemical reactions, which in turn boosts (lowers) the heat transfer gradient.

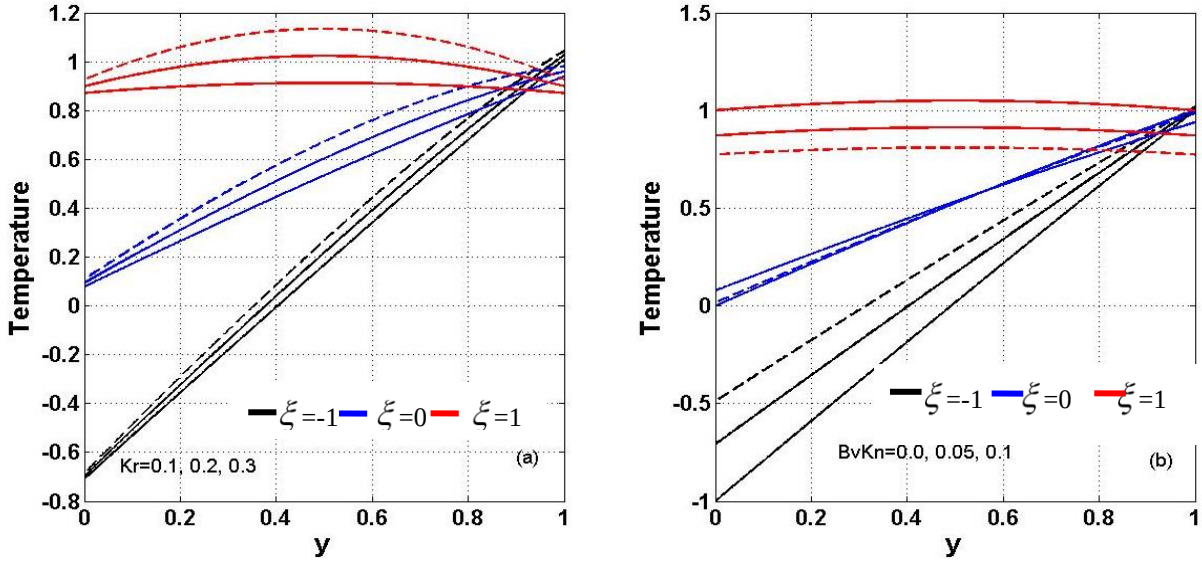

Figure 2: Temperature gradients for values of (a) K_r and (b) $\beta_v Kn$ at ξ =-1,0,1

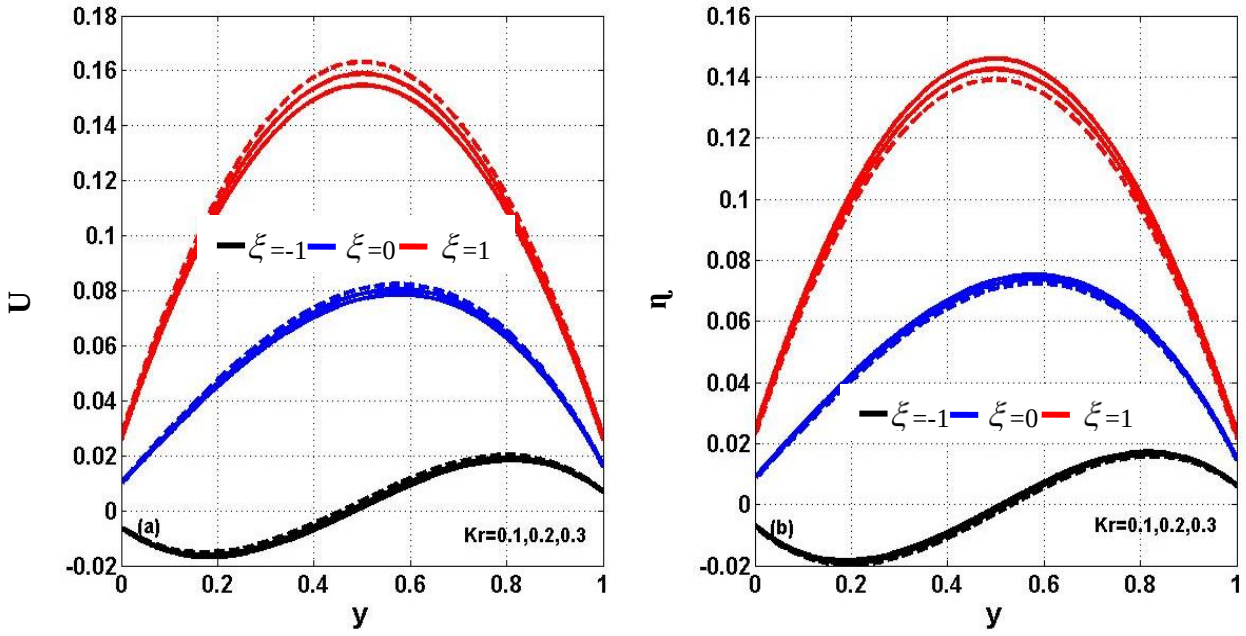

Figure 3: (a) Primary and (b) secondary velocity gradients for values of K_r at ξ =-1,0,1

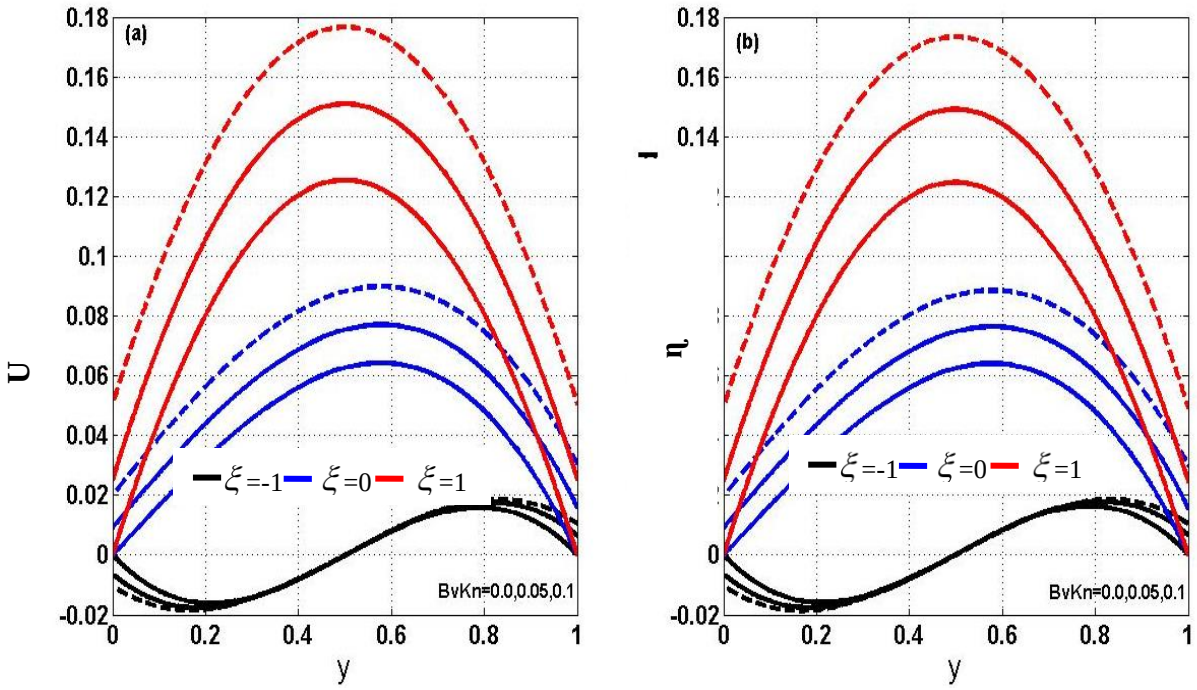

Figure 4: (a) Primary and (b) secondary velocity gradients for values of $\beta_v Kn$ atξ =-1,0,1

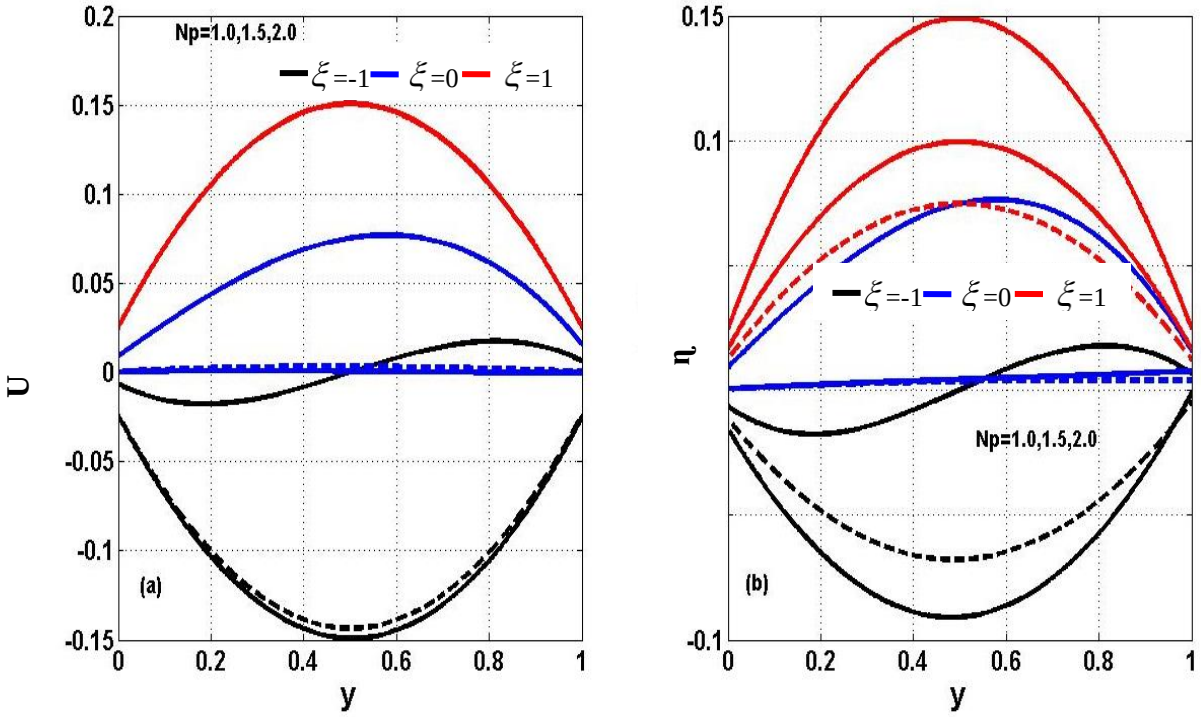

Figure 5: (a) Primary and (b) secondary flow gradients for values of Np at ξ =-1,0,1

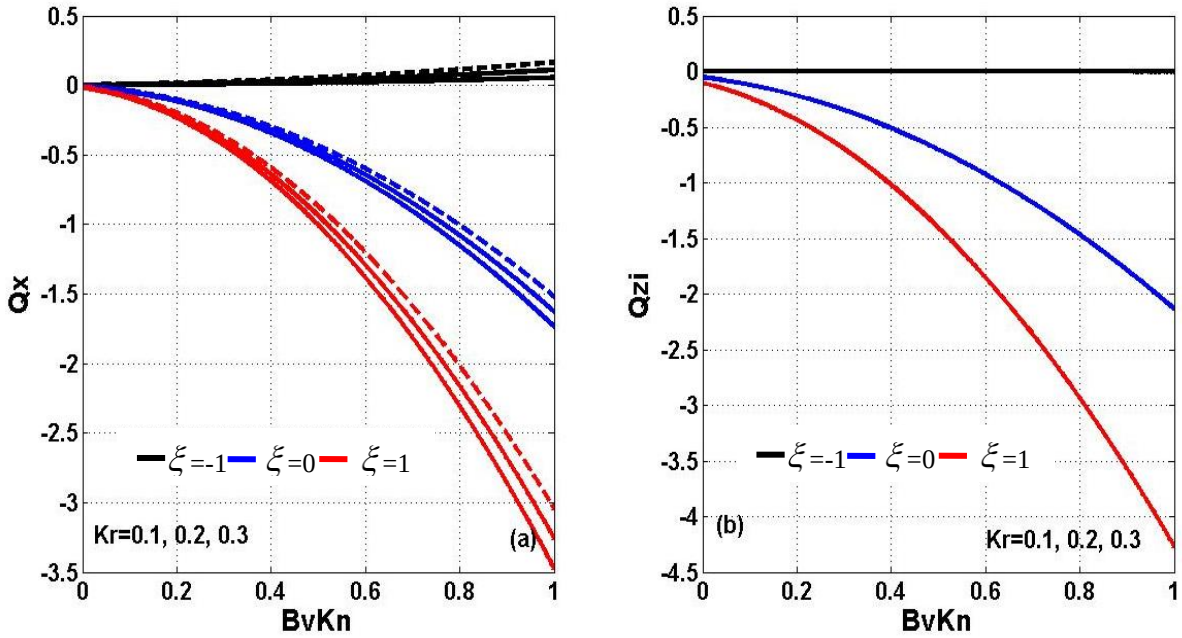

Figure 6: Volume flow rate for (a) Primary and (b) secondary flow gradients for values of K_r at ξ =-1,0,1

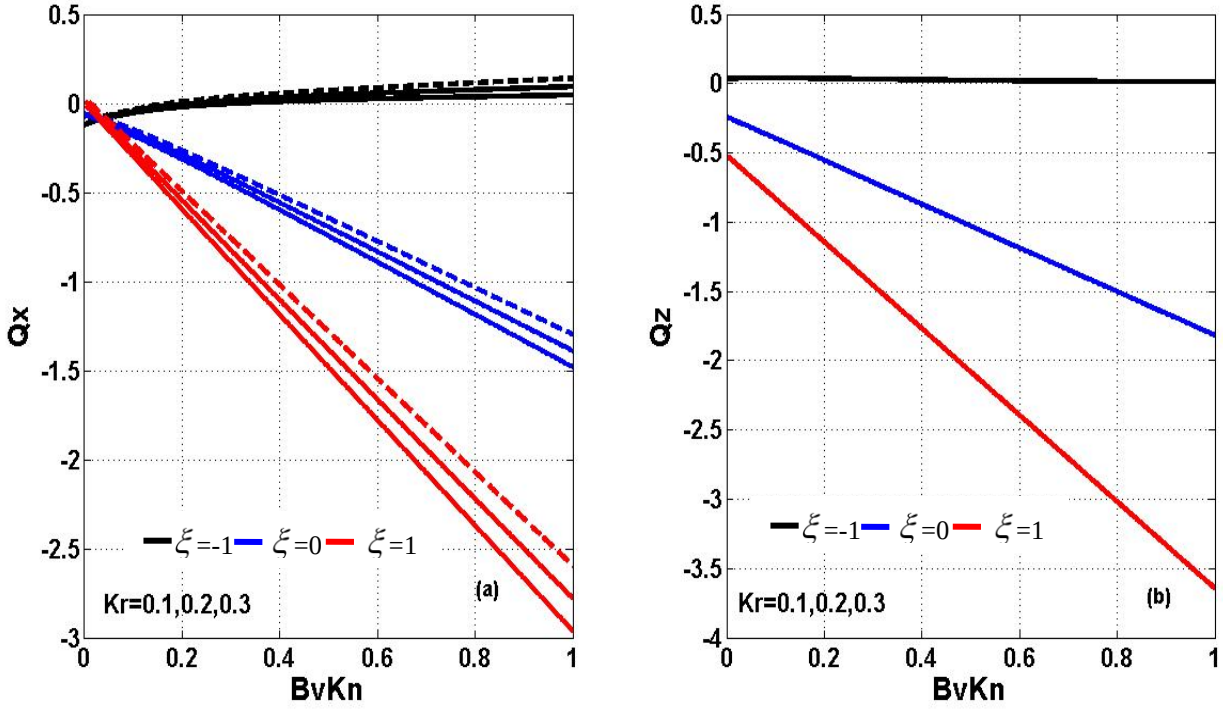

Figure 7: Skin friction at Y=0 for (a) Primary and (b) secondary flow gradients for different values of K_r at ξ =-1,0,1

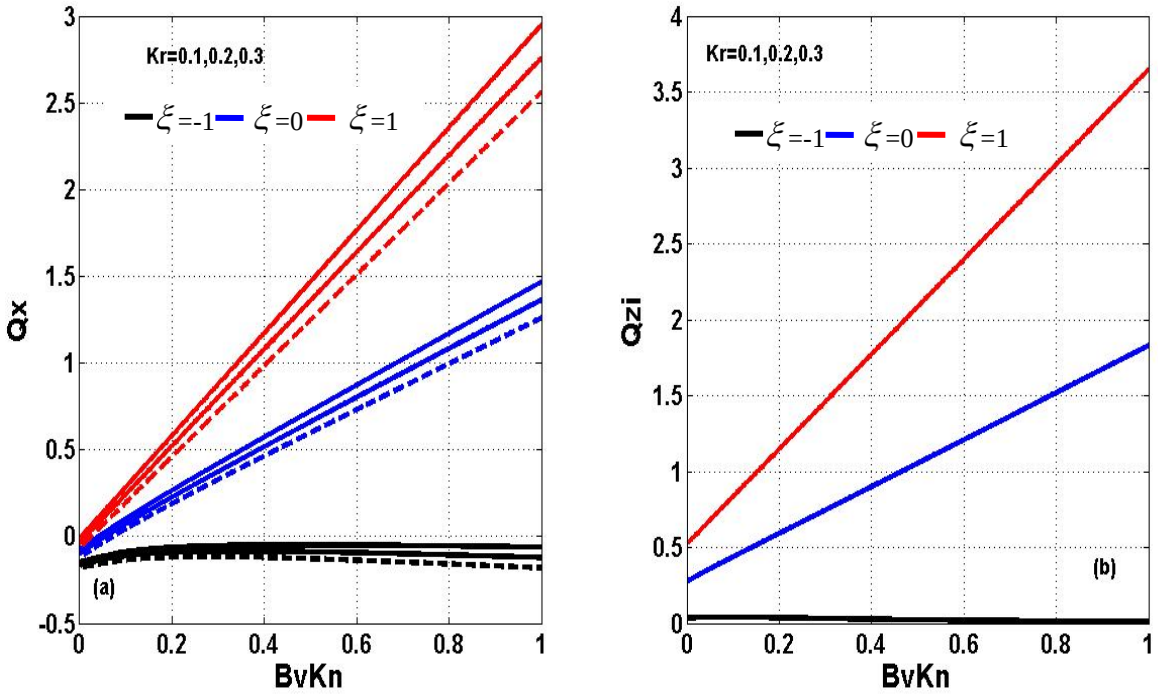

Figure 8: Skin friction at Y=1 for (a) Primary and (b) secondary flow gradients for different values of K_r at ξ =-1,0,1

ξ=-1 ξ=0 ξ=1 ξ=-1 ξ=0 ξ=1

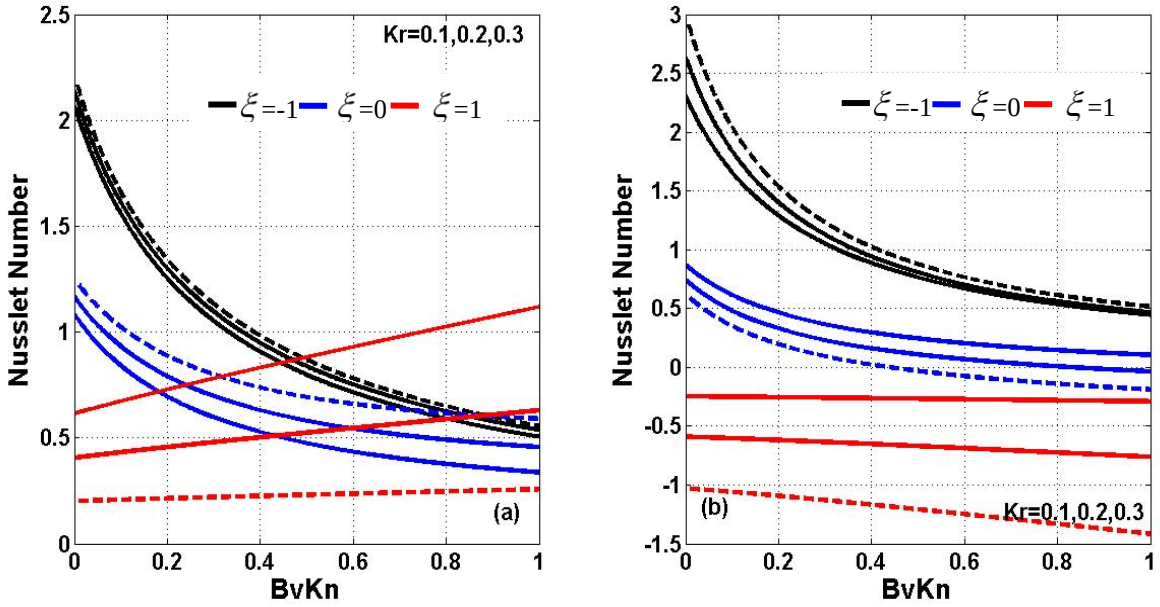

Figure 9: Nusselt number at (a) Y=0 and (b) Y=1 for different values of K_r against $\beta_v Kn$ at ξ =-1,0,1

Validation of results

For us to check the validity of the current analysis, we show the numerical computations of Jha *et al.* (2017) and the present work. As demonstrated in Tables 1 and 2, a good agreement was recorded for the complex velocity and temperature gradients.

Table 1: Numerical computations between the work of Jha *et al*. (2017) and the present analysis for complex velocity ϕ(Y) for $\xi = -1 and 0$, $\beta_v Kn$ =0.05, M=2, Np=1 as K_r approaches 0.

	Jha *et al.* (2017) ϕ(Y)		Current work ϕ(Y)	
Y	$\xi = -1$	$\xi = 0$	$\xi = -1$	$\xi = 0$
0.1	0.0070+0.0003i	0.0149+0.0021i	0.0071+0.0004i	0.0147+0.0033i
0.2	0.0069+0.0003i	0.0146+0.0021i	0.0070+0.0004i	0.0145+0.0032i
0.3	0.0068+0.0003i	0.0144+0.0020i	0.0068+0.0003i	0.0142+0.0032i
0.4	0.0067+0.0003i	0.0141+0.0020i	0.0067+0.0003i	0.0140+0.0031i

Table 2: Showing computations between the work of Jha *et al.* (2017) and the current analysis for temperature profiles θ(Y) for $\xi = -1 and 0, \beta_v Kn$ =0.05, M=2, Np=1 as K_r approaches 0.

	Jha *et al.* (2017) θ (Y)		Current work θ(Y)	
Y	$\xi = -1$	$\xi = 0$	$\xi = -1$	$\xi = 0$
0.1	0.8503	0.9251	0.8503	0.9251
0.2	0.8520	0.9260	0.8520	0.9260
0.3	0.8537	0.9268	0.8537	0.9269
0.4	0.8554	0.9277	0.8554	0.9277

CONCLUSION

A fully developed free MHD flow of an Arrhenius-controlled fluid in a micro-channel provoked by Hall current effects was performed. A closed form solutions were obtained for temperature, primary flow, secondary flow, volumetric flow, skin friction, and Nusselt number. The impacts of controlling factors such as (K_r), (Np), ($\beta_v Kn$), and (ξ) have been computed, and the results have been thoroughly discussed with the aid of various plots. The outcomes of this research could be used in biomedical engineering, the chemical and drying industries, aeronautical engineering, chemical vapor storage, and other sectors. The major outcomes from this research are highlighted below:

I. It is found out that uplifting Np, K_r and $\beta_v Kn$ parameters propel the primary and secondary flows and volume flow rate for different ascending values of ξ.

II. An upsurge in K_r and ξ parameters significantly support the temperature profile in the microchannel.

III. When Np, K_r and $\beta_v Kn$ levels are raised, the drag force effect is boosted at Y=0, while the opposite behavior is witnessed at Y=1.

IV. The amount of heat transfer peters out for higher values of K_r and ξ at both walls of the microchannel.

V. Ignoring the chemical reaction term, this present work agrees excellently with Jha's *et al*. (2017) work.

VI. The utilized method (HPM) shows a good agreement in terms of accuracy and convergence for modeling flow

REFERENCES

Al-Nimr M. A. and Khadrawi A. F. (2004).Thermal behavior of astagnant gas confined in a horizontal micro-channel as describedby the dual-phase-lag heat conduction model. Int. *J.Thermophys*.25(6):1953–1964.

Ayati Z. and Biazar J. (2015). On the convergence of Homotopy Perturbation Method. *J. Egyptian Math Soc*,.23:424-428.

Aziz A. and Shams M. (2020). Entropy generation in MHD Maxwell nanofluid flow with variable thermal conductivity, thermal radiation, slip conditions, and heat source. *AIPAdv*.10,015038.

Buonomo, B. and Manca, O. (2012). Natural Convection Flow in a Vertical Micro-Channel with Heated at Uniform Heat Flu, .*Int .J.Therm.Sci*, .49 1333-1344

Chen, C. K. and Weng, H. C. (2005). Natural convection in a vertical micro-channel. *J Heat Trans*, 127:1053-1056.

El-Aziz M. A. and Yahaya A. S. (2017). Heat and mass transfer of unsteady hydromagnetic free convection flow through porous medium past a vertical plate with surface heat flux. *J. Theoret Applied Mech. Sofia*.47 (3):25-58

Gul T, Ullah K. Bilal K. M. Alghamdi W. Asjad, M. Abdeljawad I. A. (2021). Hybrid nanofluid flow within the conical gap between the cone and the surface of a rotating disk, *Scientific. Reports,* 111180.

Gurivireddy P., Raju M., Mamatha C. B. and Varma, S. K. (2016). Thermal diffusion effect on MHD heat and mass transfer flow past a semi-infinite moving vertical porous plate with generation and chemical reaction. *Applied math*., 7 (7):638.

Hamza M. M., Ojemeri G. and Ahmad, S. K., (2023). Theoretical study of Arrhenius-controlled heat transfer flow on natural convection affected by an induced magnetic field in a microchannel, *Engineering Reports, Wiley*, DOI:10.1002/eng2.12642

Hamza, M. M. and Shuaibu A. (2022). Influence of chemical kinetic exponent on transient mixed convective hydro-magnetic flow in a vertical channel with convective boundary condition, *Journal of thermofluids*, 16:100220

He J H. (1999). Homotopy perturbation method. *Comput meth appl mech Eng* 178: 257-262.

He J H. (2000). A coupling method of a homotopy perturbation technique and a perturbation for non-linear problems. *International Journal of nonlinear mechanics*, 35:37-43.

He J H. (2003). Homotopy perturbation method: a new nonlinear analytical technique, *Appl math comput* 135:73-79.

He J H. (2006). Homotopy perturbation method for solving boundary value problems, *Physics letters A*,350, 87-88.

Jha B. K., Aina, B. an Ajiya A. T.(2014a). MHD natural convection flow in a vertical parallel plate micro-channel, *Ain shams Eng. J*,.6:289-295

Jha B. K and Aina B. (2016). Role of induced magnetic field on MHD natural convection flow in vertical microchannel formed by two electrically non-conducting infinite vertical parallel plates. *Alexandria Eng J.* 55: 2087-2097

Jha B. K. Aina B. and Joseph S. B. (2014b). Natural Convection Flow in vertical Micro-channel with Suction/Injection. J Proc Mech Eng., 228(3) :171-180

Jha B. K. and Malgwi B. P. (2019). Effects of Hall current and magnetic field inclination on hydro-magnetic natural convection flow in a micro-channel with asymmetric thermal boundary condition. *J. Therm. Sci. Eng. Appl.* 12: 031001.

Jha B. K., Aina B. and Isa S. (2015). Fully developed MHD natural convection flow in a vertical annular microchannel: an exact solution. *J. king Saudi Univ, Sci* 27: 253-259

Jha, B. K and Aina B. (2015). Mathematical modelling and exact solution of steady fully developed mixed convection flow in a vertical micro-porous-annulus. *J. AfrikaMatem-atika*, 26 :1199-1213

Jha, B. K. and Malgwi P. B. (2021). Interplay of conducting and non-conducting walls on hydromagnetic natural convection flow in a vertical micro-channel with Hall current. *Propul power Res*. 10(2): 155-168.

Jha, B. K., Aina B. and Muhammad S. A. (2015). Combined Effects of Suction/Injection and Wall Surface Curvature on Natural Convection Flow in a Vertical Annular Micro-channel, *J. ThermophysicsAeromech*,22 (2) :217-228

Jha, B. K., Malgwi P. B., and Aina B.. (2017.)Hall effects on MHD natural convection flow in a vertical micro-channel. *Alexandria Eng.J*,.2017:http://dx.doi.org/10.1016/j.aej.2017.01.038

Krishna M. V. and Chamkha A. J. (2019). Hall and ion slip effects on MHD rotating boundary layer flow of nanofluid past an infinite vertical plate embedded in a porous medium. *Results Phys.* 15: 102652.

Krishna V. M., Ahmad N. A. and Chamkha, A. J. (2020). Hall and ion slip effects on unsteady MHD free convective rotating flow through a saturated porous medium over an exponential accelerated plate, *Alexandria Eng. J.* 59 (2): 565-577.

Krishna V. M., Sravanthi C. S. and Reddy R. S. (2020). Hall and ion slip effects on MHD rotating flow of ciliary propulsion of microscopic organism through porous media. *Int. Commun. Heat Mass Trans.* 112 :104500.

Ltaifa B., D'Orazio A. and Dhahri H. (2021). Numerical analysis of mixed convection heat transfer and laminar flow in a rectangular inclined micro-channel totally filled with Water/Al2O3 Nano fluid, *J. Thermal and Analytical Calometry*, 144: 2465–2482

Ojemeri G., Omokhuale E., Hamza M. M., Onwubuya I. O. and Shuaibu A. (2023). A Computational Analysis on Steady MHD Casson Fluid Flow Across a Vertical Porous Channel Affected by Thermal Radiation Effect. *International Journal of Science for Global Sustainability*, 9(1):https://doi.org/ 10.57233/ijsgs.v9i1.393

Ojemeri, G. and Hamza, M. M. (2022): Heat transfer analysis of Arrhenius-controlled free convective hydromagnetic flow

with heat generation/absorption effect in a micro-channel, *Alexandria Eng. J*., **61**:12797-12811.

Omokhuale E. and Dange M. S. (2023). Heat absorption effect on magnetohydrodynamics(MHD) flow of Jeffery fluid in an infinite vertical plate. *FUDMA Journal of Sciences*, 7(2), 45-51

Quader A. and Alam M., ()2021. Soret and Dufour effects on unsteady free convection fluid flow in the presence of Hall current and heat flux. *J Applied math phys.* 9: 1611-1638. DOI:10:4236/ijamp.2021.97109

Rajput U S and Gupta N K (2021). Hall current and radiation effects on unsteady natural convection MHD flow with inclined magnetic field. *Applications and applied mathematics: an international journal*, 16(1),:538-548

Saeed A. and Gul T. (2021). Bi-convection casson nanofluid flow together with Darcy-Forchheimer due to a rotating disk with thermal radiation and arrhenius activation energy, *SN Applied Sciences*, 3,78:1-19.

Sutton G. and Sherman A. (1965). Engineering Magneto-hydrodynamics, McGraw-Hill, New York.

Uygun, N. and Ahmad H. T. (2022). Botmart. The effect of Hall parameter on the MHD fluid flow and heat transfer induced by uniform radial electric field due to a shrinking rotating disk. *Case studies in thermal engineering*, vol 37,. 102222

Weng, H. C. and Chen, C. K. (2009). Drag reduction and heat transfer enhancement over a heated wall of a vertical annular micro-channel, *International Journal of. Heat and Mass Transfer,* 52:1075–1079

Zainal N A, Nazar R., Naganthran K and Pop I. (2021). Heat generation/absorption effect on MHD flow of hybrid nanofluid over bidirectional exponentially stretching/shrinking sheet, *Chinese journal of physics*, 69: 118-133.

Nomenclature

B_0=constant magnetic flux density
g=gravitational acceleration
b= channel width
C_pC_v=specific heats at constant pressure and constant volume respectively
f_pf_v =thermal and tangential momentum accommodation coefficients, respectively
In=fluid -wall interaction parameter
Kn =Knudsen number a/b
Kr=chemical reaction parameter
Np=Hall current parameter
Γ =dimensionless volume flow rate
M= Hartmann number
Pr=Prandtl number
Nu=dimensionless heat transfer rate
Ac=activation energy
T=Temperature of the fluid
T_0=Reference temperature
u=velocity component in x direction
U=dimensionless velocity

Greek letters

β =thermal expansion coefficient
$\beta_t\beta_v$=dimensionless variables
μ =dynamic viscosity
α =thermal diffusivity
γ_s= ratios of specific heats (C_pC_v)
ξ =wall-ambient temperature difference ratio
σ =electrical conductivity of the fluid
ρ = density
v=fluid kinematic viscosity

APPENDIX

$$A_0 = \xi + \frac{BnKnIn(1-\xi)}{1+2BnKnIn}, A_1 = \frac{(1-\xi)}{1+2BnKnIn},$$

$$A_0 = \xi + \frac{BnKnIn(1-\xi)}{1+2BnKnIn}, A_1 = \frac{(1-\xi)}{1+2BnKnIn}, A_2 = BnKnInA_3$$

$$A_3 = \frac{\lambda BnKnIn(s_4 - s_5 + s_6) + \lambda(s_1 - s_2 + s_3)}{1+2BnKnIn}, A_4 = BnKnInA_5,$$

$$-BnKnIn(-s_{20} + s_{21} - s_{22} - s_{23} + s_{24} - s_{25} + s_{26} - s_{27} + s_{28} - s_{29} + s_{30} + s_{31})$$
$$+K_r(4K_r - 2A_cK_r)(s_8 - s_9 + s_{10}) + s_{11}(4K_r - 2A_cK_r)(s_{12} - s_{13} + s_{14}) + s_{15}(4K_r - 2A_cK_r)$$

$$A_5 = \frac{-{K_r}^2(s_{16} - s_{17} + s_{18}) - s_{19}}{1+2BnKnIn}$$

$$R_1 = \frac{w_{15} - w_{13}}{w_{11} - w_{12} - w_{14} + \frac{w_7B_vKn}{N_p} + \frac{w_7}{N_p}}, R_2 = B_vKnR_1 - w_3, R_3 = \frac{w_3}{2w_5} + w_8B_vKn - \frac{R_1w_4}{w_5}$$

$$R_4 = B_vKnR_3, R_5 = \frac{w_{64}}{w_{63}}, R_7 = w_{29} + R_5w_{30}, R_6 = w_{24}R_7 - B_vKnR_5 + w_{25}, R_8 = B_vKnR_7,$$

$$J_2 = (\frac{A_1B_vkn}{2} + A_0B_vkn + \frac{A_1}{6} + \frac{A_0}{2})/(1+2B_vkn), J_3 = B_vknJ_2,$$

$$J_4 = (-w_{65} - w_{69} - w_{75} - w_{70}B_vkn - w_{74}B_vkn)./(1+2B_vkn), J_5 = B_vknJ_4$$

$$w_1=\frac{M^2}{1+N_p^2},\quad w_2=N_p^2(w_1^{\,2}+1),\quad w_3=A_0-A_1B_vKn,\quad w_4=R_1(B_vKn+1/6+B_vKn^2),$$

$$w_5=1+2B_vKn,\quad w_6=\frac{w_3(1/2+B_vKn)}{w_5},\ w_7=\frac{w_4}{w_5},\quad w_8=\frac{A_0+A_1}{N_pw_1},$$

$$w_9=-\frac{w_3}{2}+w_6+B_vKnw_6,\quad w_{10}=-w_3+w_6,\quad w_{11}=\frac{R_1(1+B_vKn)}{N_pw_1}$$

$$w_{12}=R_1(\frac{1}{6N_p}+\frac{B_vKn}{2N_p}),\quad w_{13}=-\frac{w_3}{N_pw_1}+w_8-\frac{w_9}{N_p},\quad w_{14}=\frac{B_vKn}{2N_p}+\frac{B_vKn^2}{N_p}-\frac{B_vKn}{w_1N_p}$$

$$w_{15}=-\tfrac{B_vKnA_1}{N_pw_1}+\tfrac{w_{10}B_vKn}{N_p},w_{16}=2w_1(\tfrac{R_1}{120}+\tfrac{R_2}{24}),w_{17}=w_2(\tfrac{R_1}{5040}+\tfrac{R_2}{720}+\tfrac{R_3}{120}+\tfrac{R_4}{24}),$$
$$w_{18}=w_1(\frac{A_0}{24}+\frac{A_1}{120}),w_{19}=2w_1(\frac{R_1}{24}+\frac{R_2}{6}),w_{20}=w_2(\frac{R_1}{720}+\frac{R_2}{120}+\frac{R_3}{24}+\frac{R_4}{6}),w_{21}=w_1(\frac{A_0}{6}+\frac{A_1}{24}),$$
$$w_{22}=w_{16}-w_{17}+w_{18},w_{23}=B_vKn(w_{19}-w_{20}+w_{21}),w_{24}=2w_1B_vKnR_{7,}$$
$$w_{25}=-B_vknA_3-A_2,w_{26}=\frac{w_{24}}{2}+w_{24}B_vkn+w_5$$

$$w_{42}=w_2(\frac{R_1}{24}+\frac{R_2}{6}+\frac{R_3}{2}+R_4),w_{43}=w_1(A_0+\frac{A_1}{2}),w_{44}=1+A_0+\frac{A_1}{2},w_{45}=A_c(A_0^2+A_0A_1+\frac{A_1^2}{3}),$$
$$w_{46}=2(A_0^2+A_0A_1+\frac{A_1^2}{3}),w_{47}=2w_1(\frac{R_1}{24}+\frac{R_2}{6}),w_{48}=w_2(\frac{R_1}{720}+\frac{R_2}{120}+\frac{R_3}{6}+\frac{R_4}{2}),w_{49}=w_1(\frac{A_0}{6}+\frac{A_1}{24})$$
$$w_{50}=w_{31}-w_{32}+w_{33},w_{51}=(-K_r(w_{34}-w_{35}+w_{36})+w_{37})./w_1N_p,w_{52}=w_{38}-w_{39}+w_{40},$$
$$w_{53}=w_{41}-w_{42}+w_{43},w_{54}=(-K_r(w_{44}-w_{45}+w_{46})+A_3)./w_1N_p,w_{55}=w_{47}-w_{48}+w_{49},$$
$$w_{26}=\frac{w_{24}}{2}+w_{24}B_vkn+w_{25},w_{27}=w_{23}-w_{22}-w_{25}B_vkn,w_{28}=B_vkn^2-\frac{1}{6},w_{29}=\frac{w_{27}}{w_{26}},$$
$$w_{30}=\frac{w_{28}}{w_{26}},w_{31}=2w_1(\frac{R_1}{6}+\frac{R_2}{2}),w_{32}=w_2(\frac{R_1}{120}+\frac{R_2}{24}+\frac{R_3}{6}+\frac{R_4}{2}),w_{33}=w_1(\frac{A_0}{2}+\frac{A_1}{6})w_{34}=\frac{1}{2}+\frac{A_0}{2}+\frac{A_1}{6},$$
$$w_{35}=A_c(\frac{A_0^2}{2}+\frac{A_0A_1}{3}+\frac{A_0^2}{2}),w_{36}=2(\frac{A_0^2}{2}+\frac{A_0A_1}{3}+\frac{A_0^2}{2}),w_{37}=A_3+A_2,w_{38}=2w_1(\frac{R_1}{120}+\frac{R_2}{24}),$$
$$w_{39}=w_2(\frac{R_1}{5040}+\frac{R_2}{720}+\frac{R_3}{120}+\frac{R_4}{24}),w_{40}=w_1(\frac{A_0}{24}+\frac{A_1}{120}),w_{41}=2w_1(\frac{R_1}{2}+R_2),$$

$$w_{56}=\frac{1+w_{24}w_{30}-B_vkn}{w_1N_p},w_{57}=(w_{50}+w_{24}w_{29}+w_{25})./w_1N_p,w_{58}=(w_{52}+\frac{w_{24}w_{29}}{2}+\frac{w_{25}}{2}+w_5w_{29})./N_p,$$
$$w_{59}=\frac{1}{2N_p}+\frac{w_{24}w_{30}}{2N_p}-\frac{B_vkn}{2N_p}+\frac{w_5w_{30}}{N_p},w_{60}=-\frac{w_{53}B_vkn}{2N_p}-w_{54}B_vkn,w_{61}=B_vkn(w_{55}+w_{24}w_{29}+w_{25}+w_{29})./N_p,$$
$$w_{62}=B_vkn(\frac{1}{2}+w_{24}w_{30}-B_vkn+w_{30})./N_p,w_{63}=w_{56}-w_{59}+\frac{B_vkn}{2N_p}-w_{62},w_{64}=w_{60}+w_{61}-w_{57}-w_{51}+w_{58},$$
$$w_{65}=M_1^2(-\frac{A_1}{120}-\frac{A_0}{24}+\frac{J_2}{6}+\frac{J_3}{2}),w_{66}=\frac{1}{24}+\frac{A_0}{24}+\frac{A_1}{120},w_{67}=A_c(\frac{A_0^2}{24}+\frac{A_0A_1}{60}+\frac{A_1^2}{360}),w_{68}=2(\frac{A_0^2}{24}+\frac{A_0A_1}{60}+\frac{A_1^2}{360}),$$
$$w_{69}=-\frac{A_3}{6}-\frac{A_2}{2},w_{70}=M_1^2(-\frac{A_1}{24}-\frac{A_0}{6}+\frac{J_2}{2}+J_3),w_{71}=\frac{1}{6}+\frac{A_0}{6}+\frac{A_1}{24},w_{72}=A_c(\frac{A_0^2}{6}+\frac{A_0A_1}{12}+\frac{A_1^2}{60}),$$
$$w_{73}=2(\frac{A_0^2}{6}+\frac{A_0A_1}{12}+\frac{A_1^2}{60}),w_{74}=-\frac{A_3}{2}-A_2,w_{75}=K_r(w_{66}-w_{67}+w_{68}),w_{76}=K_r(w_{71}-w_{72}+w_{73})$$